

## Superconducting properties of $VN_x$ sputtered films including spin fluctuations and radiation damage of stoichiometric VN

K. E. Gray, R. T. Kampwirth, and D. W. Capone II

*Materials Science Division, Argonne National Laboratory, Argonne, Illinois 60439*

R. Vaglio

*Dipartimento di Fisica, Universita degli Studi di Salerno, I-84100 Salerno, Italy*

J. Zasadzinski

*Illinois Institute of Technology, Chicago, Illinois 60616*

(Received 15 September 1987; revised manuscript received 22 December 1987)

We have made well-ordered, stoichiometric films of VN using reactive sputtering and studied the effects of disordering due to deviations from stoichiometry and radiation damage. An unexpected local minimum of  $T_c$  for the well-ordered, stoichiometric VN was found. The principal result was that the peak in  $T_c$  for substoichiometric  $VN_{0.96}$  can be shown to be consistent with a competition between spin fluctuations and electron-phonon coupling, but we find the effect of the former is smaller than previously predicted. The superconducting properties measured in radiation-damaged VN have been extrapolated to pure, stoichiometric VN.

### I. INTRODUCTION

We have made well-ordered stoichiometric films of VN using reactive dc triode sputtering. These films have a residual resistivity ratio,  $r_R \equiv \rho_{300}/\rho_{10}$  of 8–9, where  $\rho_{300}$  and  $\rho_{10}$  are the resistivities at 300 K (room temperature) and 10 K, respectively. We have also studied the effect of disorder, caused by both  $\alpha$ -particle irradiation and deviations from stoichiometry. There is a local minimum in the superconducting transition temperature,  $T_c$ , versus N concentration,  $x$ , at the stoichiometric ( $x=1$ ) composition, and a maximum  $T_c$  of 8.9 K for a lower concentration,  $x_m$ , which is estimated to be about 0.96 from the lattice constant.

This nonmonotonic variation of  $T_c$  is shown to be consistent with the competing effects on  $T_c$ , as  $x$  increases, with the following: (i) an increasing electron-phonon coupling and bare electronic density of states (of one spin),  $N(0)$ , the latter recently calculated<sup>1</sup> as a function of  $x$ ; and (ii) an increasing Stoner factor, and hence spin fluctuations, as measured<sup>2</sup> by the magnetic susceptibility as a function of  $x$ . Thus we have determined  $T_c(x)$  based on the McMillan equation<sup>3,4</sup> modified to include spin fluctuations. Comparing this calculation with our measured  $T_c(x)$  shows consistency with the presence of spin fluctuations, but that they exhibit a smaller effect than previously predicted.<sup>5</sup> Note that this prediction<sup>5</sup> was based on first-principles calculations of the phonon and spin fluctuation interactions in VN, whereas our model relies heavily on experimentally measured quantities to determine the parameters.

For stoichiometric films disordered by  $\alpha$ -particle irradiation,  $T_c$  also increases initially, reaching a broad maximum at 9.3 K for  $3-10 \times 10^{16}$   $\alpha/cm^2$ . Based on these measurements, various properties have been extrapolated

to pure, stoichiometric VN:  $T_c = 7.8 \pm 0.1$  K; the upper critical field slope,  $H'_{c2} \equiv -(dH_{c2}/dT)_{T_c} = 600 \pm 200$  Oe/K; and the electron-phonon renormalized Fermi velocity,  $\langle v_F^* \rangle = 2.4 (\pm 0.4) \times 10^7$  cm/sec.

Section II covers sample preparation and characterization, including superconducting properties. A crucial part of the analysis is the identification of the resistive transition of the stoichiometric compound since a minority substoichiometric component is always found. This is described in Sec. III and spin fluctuations are covered in Sec. IV. Measurements after  $\alpha$ -particle irradiation are described in Sec. V: these add to our understanding of the effects of disorder on VN. A general discussion and summary follows in Sec. VI.

### II. SAMPLE PREPARATION AND CHARACTERIZATION

All films were made by reactive dc sputtering using a Plasmax triode source which allowed independent manipulation of the discharge current and target potential (typically 400–700 V). Approximately 75 films were deposited onto polished, single-crystal sapphire substrates with two different orientations, i.e., the sapphire  $c$ -axis parallel ( $0^\circ$ ) or perpendicular ( $90^\circ$ ) to the film normal. Optimum substrate temperature for well-ordered films was 500–600°C, measured by mounting a Chromel-Alumel thermocouple to the surface of an adjacent substrate on the heater block. The stainless-steel vacuum chamber was pumped sequentially by an oilless rotary pump, liquid-nitrogen-cooled sorption pump, and a closed-cycle helium cryopump which provided a hydrocarbon-free environment. After bakeout the typical residual pressure in the chamber prior to sputtering was  $2 \times 10^{-7}$  Torr with the heater at 600°C. High-purity (99.999%) argon was

injected directly into the Plasmax source, whereas the  $N_2$  gas was bled in via one of the chamber ports, both gases being pumped through a liquid-nitrogen-cooled orifice on the cryopump. Typical pressures for the Ar and  $N_2$  were 6 and 0.1–4 mTorr, respectively, as measured by a Baratron absolute-pressure manometer. The vanadium target (0.75 in. diam.) was prepared by melting VP-grade pellets from Materials Research Corporation (MRC) in an ultrahigh vacuum electron-beam hearth. Because of the sensitivity of  $T_c$  to oxygen contamination in transition metals and their compounds, it is important to maintain as low a partial pressure of  $O_2$  as possible. A stringent test of  $O_2$  contamination for any sputtering system is to deposit pure V at moderate rates and check  $T_c$ . Our deposition of V films onto unheated substrates at rates of 3 Å/sec resulted in  $T_c$  values near 5.0 K, close to the bulk value of 5.3 K. We believe this indicates that there are no significant problems with oxygen contamination in our films. Typical deposition rates of the VN films were 40–100 Å/min and their thicknesses were  $\sim 4000$ –5000 Å.

Figure 1 shows the variation of resistance ratio,  $r_R$ , as a function of nitrogen partial pressure,  $P_N$ , for films sputtered using the conditions outlined above. All parameters, including sputtering voltage, were identical except  $P_N$  and the sputtering rate,  $R$ , which decreased from  $\sim 100$  to  $\sim 45$  Å/min as  $P_N$  increased from 0.1 to 4 mTorr. This decrease in rate is presumably due to nitriding of the target surface which reduces the sputter yield. Since high values of  $r_R$  imply well-ordered, single-phase films, the data of Fig. 1 are interpreted to show two distinct phases of the V-N system, at  $P_N \sim 0.3$  and 2.6 mTorr. Films made near the peak in  $r_R$  at  $P_N = 2.6$  mTorr were analyzed by transmission electron micros-

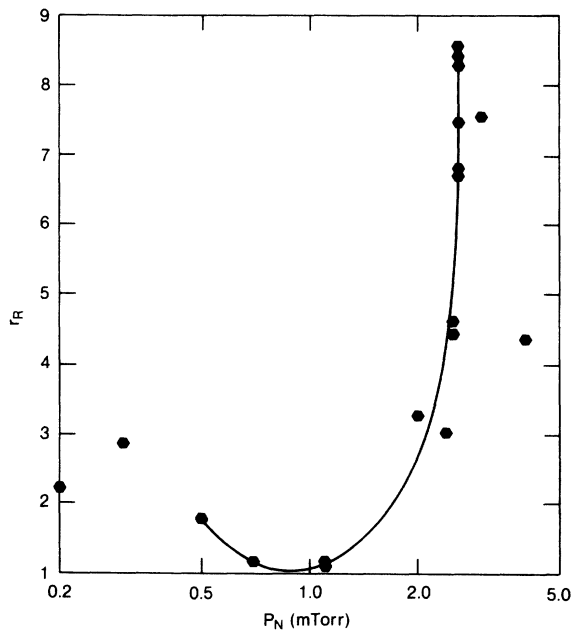


FIG. 1. The measured resistance ratio,  $r_R$ , as a function of partial pressure of N during sputtering. Ordered phases are indicated for  $P_N \sim 0.3$  and 2.6 mTorr.

copy. No evidence for defects nor grain boundaries was found over distances of about 1  $\mu\text{m}$ .

Conventional x-ray diffraction for samples made on  $0^\circ$  sapphire substrates at  $P_N \gtrsim 1$  mTorr showed only a single, sharp line (see Ref. 6) corresponding to reflections from the (111) plane of the fcc structure of VN. This allowed a determination of the lattice constant, but for  $90^\circ$  sapphire substrates, the single line was not usually observable due to imperfect cutting of the sapphire. For this reason, x-ray data are unavailable for the V-N phase found in films with  $P_N \approx 0.3$  mTorr. However, this phase can be presumed to be the hexagonal  $\beta$ -VN phase which is known<sup>7</sup> to exist over the composition limits  $0.35 \leq x \leq 0.49$ .

Measurements of the superconducting transition temperature,  $T_c$ , for several representative samples are shown in Fig. 2. These confirm that the phase found with  $P_N \sim 2.6$  mTorr is VN with  $T_c \sim 8$ –9 K. All samples with  $P_N < 1$  mTorr were not superconducting above 5 K, although the sample with  $P_N = 0.7$  mTorr exhibited a decrease in resistance for  $T \lesssim 7.5$  K, likely indicating a two-phase film. Note that the transition widths in Fig. 2 are determined between the 1% and 99% points on the resistive transitions.

A plot of transition width,  $\Delta T_c$ , against the average,  $\bar{T}_c$ , is shown in the inset of Fig. 2 for a larger set of samples. It shows the usual, expected behavior that  $\Delta T_c$  is a minimum for the highest  $T_c$  sample, which was made at  $P_N = 2$  mTorr. However, that sample has  $r_R = 3.27$  and is clearly not one of the stoichiometric, well-ordered samples found at the peak of  $r_R$ , which were made at  $P_N \sim 2.6$  mTorr.

From x-ray diffraction studies on VN, it is generally accepted<sup>2,7–10</sup> that the lattice constant decreases approximately linearly with nitrogen vacancies ( $1-x$ ). However, there is no general consensus on the exact dependence, so we are reluctant to use our single x-ray diffraction peak to assign a N concentration to each film. We can use the rate of decrease found in bulk studies to

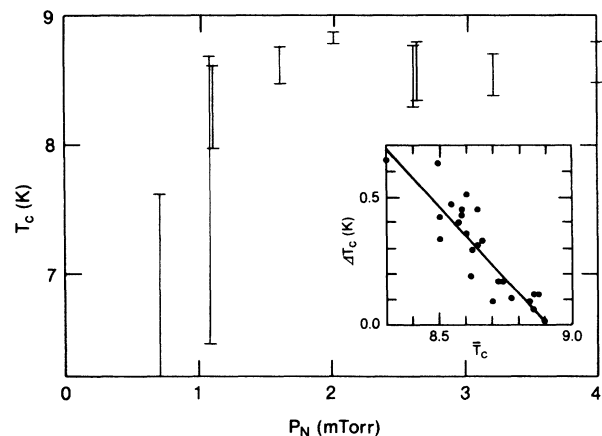


FIG. 2. The superconducting transition temperatures for various samples as a function of  $P_N$ . The widths represent 1% to 99% of the resistive transition and are plotted against average  $T_c$  in the inset for a larger number of samples.

estimate the N concentration for the peak in  $T_c$  to be at  $x \simeq 0.96$ .

The discrepancy between  $\Delta T_c$  and  $r_R$  is even more dramatic when a magnetic field is applied. Figure 3 shows a comparison of resistive transitions in various applied fields between the highest  $T_c$  sample (lower curves) and a stoichiometric sample with large  $r_R$  (upper curves). The  $\Delta T_c$  increases much more dramatically with field for the stoichiometric sample. In Fig. 4, another stoichiometric sample ( $r_R=8$ ) is shown before (lower curves) and after (upper curves) irradiation with  $5.6 \times 10^{16} \text{ } \alpha/\text{cm}^2$ . The disordering effects of the irradiation ( $r_R$  decreased to 1.7) also clearly sharpen the transition (and increase  $T_c$  as well). This behavior is certainly anomalous with respect to usual superconductors and will be dealt with in the next section.

In principle, the measured properties should be plotted against the composition,  $x$ , of the various samples. However, since we could not determine  $x$  in any satisfactory manner, we rely rather on  $r_R$  as an intrinsic property of the material at a given  $x$ . The compositions should be closely related to the relative arrival rates of N and V atoms at the substrate during deposition. This is conveniently measured by the ratio of  $P_N$  to the sputtering rate,  $R$ , and is shown in Fig. 5 as a function of  $(r_R - 1)^{-1}$ .

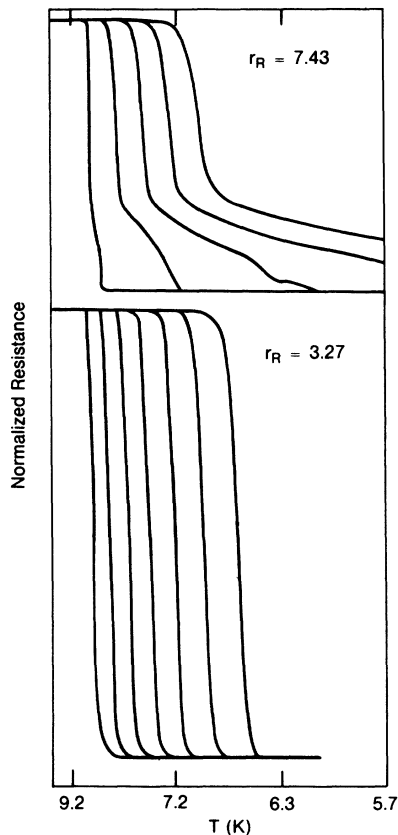


FIG. 3. Resistive transitions in various applied fields for two samples. Note the reversed nonlinear temperature scale. Upper: stoichiometric sample near the peak in  $r_R$  (from left  $H=0, 5, 10, 15, 20$  kG); lower: substoichiometric sample near the peak in  $T_c$  (from left  $H=0, 5, 10, 15, 20, 25, 30$  kG).

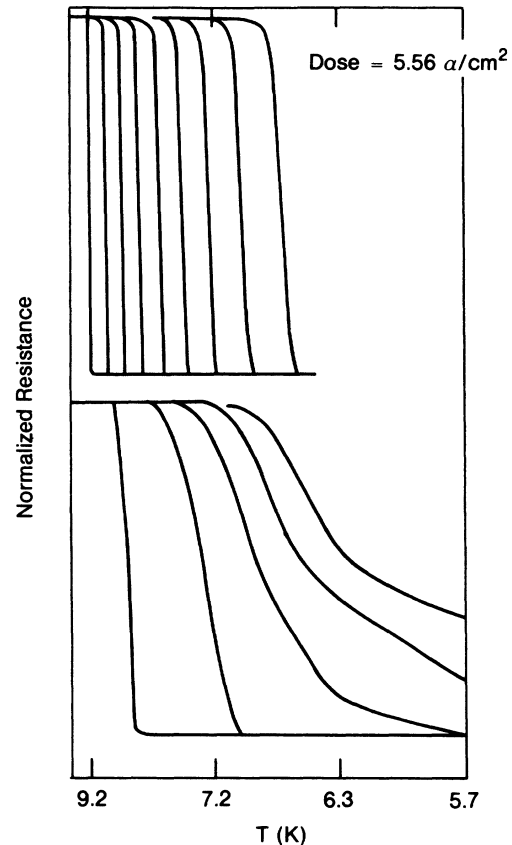


FIG. 4. Resistive transitions in various applied fields for the same sample. Note the reversed nonlinear temperature scale. Upper: after irradiation with  $5.56 \text{ } \alpha/\text{cm}^2$  (from left  $H=0, 5, 10, 15, 20, 25, 30, 35, 40$  kG); lower: before irradiation (from left  $H=0, 5, 10, 15, 20$  kG).

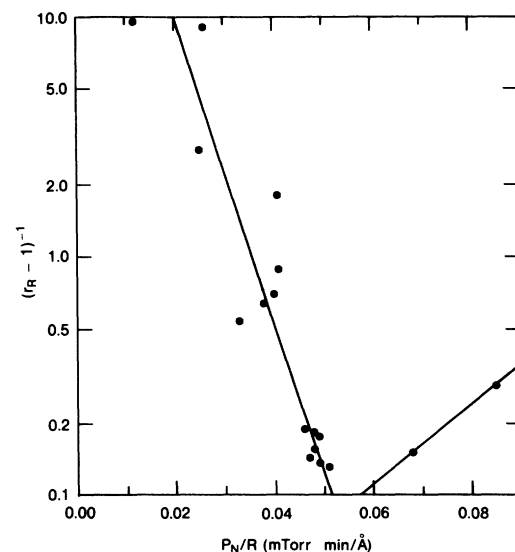


FIG. 5. The variation of  $(r_R - 1)^{-1}$  with ratio of  $P_N$  to sputtering rate,  $R$ , which measures the relative arrival rate of N to V atoms at the growing film surface during sputtering. Stoichiometric VN occurs for  $P_N/R \sim 0.05 \text{ mTorr min}/\text{Å}$ .

Note that  $(r_R - 1)^{-1}$  is an increasing function of disorder which is proportional to the normal state resistivity,  $\rho_N$ , assuming Matthiessen's rule and the expected independence on disorder of the temperature-dependent resistivity. The scatter in Fig. 5 is primarily due to uncertainties in  $R$ , but the data indicate that stoichiometric VN is found for  $P_N/R \sim 0.05$  mTorr  $\cdot$  min/ $\text{\AA}$ . Also it appears more difficult to obtain significant N excess (interstitials) as compared to deficiencies (vacancies).

For the superconducting properties, the normal state resistivity,  $\rho_N$ , is the more appropriate intrinsic parameter for each film. In a number of cases with particularly favorable geometry,  $\rho_N$  was measured, and the results, which span the total range of  $\rho_N$  values, are shown in Fig. 6 (together with a data point from Ref. 9). They fit the unexpected empirical dependence:

$$\rho_N = 20 \mu\Omega \text{ cm} (r_R - 1)^{-0.586}. \quad (1)$$

The deviation from the inverse dependence (exponent = -1), expected from Matthiessen's rule in the clean limit, is unclear, and in addition, no convincing evidence for a saturation associated with maximum metallic resistivity<sup>6,11</sup> in the dirty limit is found. Perhaps we have not achieved either of these limits in our range of  $\rho_N$  values. In any case, Eq. (1) does allow us to determine values of  $\rho_N$  for all films in which  $r_R$  was measured.

In Fig. 7 the superconducting transition temperatures are plotted against  $\rho_N$ . The indicated transition widths again represent the 1% and 99% points on the resistive transitions. As in Fig. 2, the narrow, high- $T_c$  transitions occur in substoichiometric compounds with  $\rho_N \sim 15$ – $20 \mu\Omega \text{ cm}$ . The solid line results from the analysis of spin fluctuations in Sec. V and will be discussed there.

For the reasons given in the next section, the critical field slope  $H'_{c2}$  ( $\equiv -dH_{c2}/dT$  at  $T_c$ ) is measured on the foot (1% point) of each resistive transition, and perpendicular fields are used to avoid surface superconductivity. Contrary to the  $T_c$  behavior,  $H'_{c2}$  increases monotonically with  $\rho_N$  and is shown in Fig. 8. The dashed line represents the linear increase of  $H'_{c2}$  with  $\rho_N$  which is expected if the experimental electronic specific heat coefficient is put in the theoretical Ginzburg-Landau-

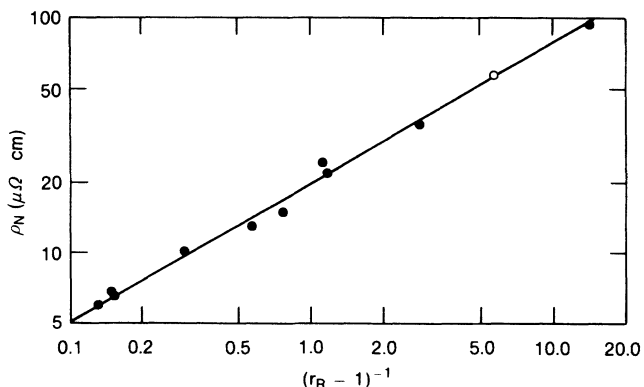


FIG. 6. The variation of measured  $\rho_N$  against  $(r_R - 1)^{-1}$  for a series of "as-made" films. The open circle is from Ref. 9.

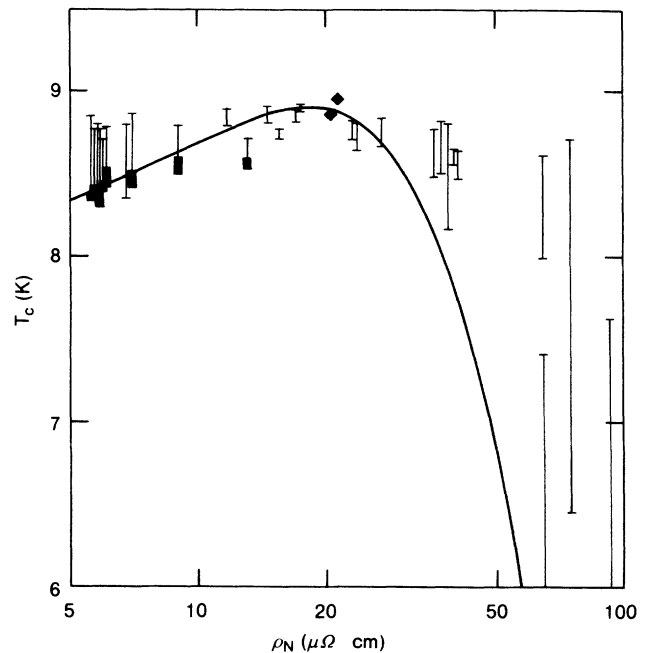


FIG. 7. The superconducting resistive transitions (widths are 1% to 99% points) as a function of  $\rho_N$ . For the low  $\rho_N$  films, the width of the foot of the transition, which represents the majority component of these well-ordered films, is shown by the solid rectangles. Diamonds are midpoints in samples for which the entire transition was not recorded. The solid line is the result of a model calculation including spin fluctuations in which  $S(x=1)=3.5$ . The peak in  $T_c$  at  $x=0.96$  is plotted at  $\rho_N = 18 \mu\Omega \text{ cm}$ .

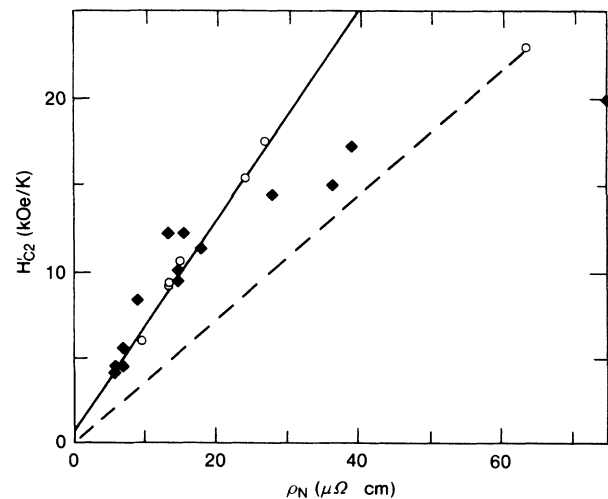


FIG. 8. Variation of the upper critical field slope as a function of  $\rho_N$  for "as-made" samples (diamonds) and radiation damaged samples (open circles). The solid line is a guide to the eye. The dashed line is the result expected from the GLAG theory using the experimental Sommerfeld constant.

Abrikosov-Gorkov (GLAG) expression:<sup>12</sup>

$$H'_{c2} = H'_{c2}(0) + b\rho_N\gamma, \quad (2)$$

where  $H'_{c2}(0)$  is the clean limit ( $\rho_N \rightarrow 0$ ) value in units of Oe/K,  $\rho_N$  is in  $\mu\Omega$  cm,  $\gamma$  is the experimental Sommerfeld constant<sup>13,14</sup> of  $8.64 \times 10^3$  ergs/cm<sup>3</sup>/K<sup>2</sup>, and  $b = 4.48 \times 10^4$  for the dirty limit if strong coupling is neglected.<sup>12</sup> Most of the data fall above this line, however the agreement improves for  $\rho_N > 30 \mu\Omega$  cm.

### III. FILM NUCLEATION MODEL FOR THE RESISTIVE FOOT

In this section a model is presented to explain the anomalous behavior of the resistive transition width,  $\Delta T_c$ , reported in the previous section. We found a minimum  $\Delta T_c$  and a maximum  $T_c$  of 8.9 K for the substoichiometric compound (i.e., VN<sub>x</sub> with  $x = x_m < 1$  which is necessarily disordered), whereas  $\Delta T_c$  increased for the most well ordered (highest  $r_R$ ), presumably stoichiometric samples, as well as for  $x < x_m$ . In addition, the disorder introduced by progressive radiation damage of the well-ordered stoichiometric VN led to sharper transitions with smaller  $\Delta T_c$  and higher  $T_c$ . This is clearly anomalous compared to usual superconductors in which the highest  $T_c$  and narrowest  $\Delta T_c$  occur for the well-ordered stoichiometric compound. Therefore the basis of our model involves two unusual occurrences: (i) that  $T_c$  of VN<sub>x</sub> exhibits a local minimum for the stoichiometric ( $x = 1$ ) compound and a maximum for the substoichiometric ( $x = x_m < 1$ ) compound, for example, see the solid curve in Fig. 7; and (ii) that a minority component, with higher  $T_c$  than the majority phase for  $x \approx 1$ , exists but does not percolate along the length of the film.

It is easy to see that such a minority component is both necessary and sufficient to obtain the observed multiple resistive transitions. However, the broadened, multiple resistive transitions shown in Figs. 3 and 4 do not result from a trivial macroscopic variation of the film properties along the length of the film being measured. To prove this, resistivity measurements using four closely spaced (0.6 mm, compared to sample lengths of  $\sim 10$  mm) contacts were performed at many locations across the surface of several of the films. These showed uniform resistivity within 2%, and included one of the cleanest films which might be expected to be the least homogeneous based on the above discussion and resistive transitions. We suggest instead that the minority component is created, for example, in the initial stages of the film growth, during which the V atoms coalesce into islands due to their high surface mobility at the substrate temperature of 500°C. Because the total area of the isolated islands is necessarily less than the total substrate area, the rate of arrival of V atoms is enhanced compared to the bulk of the film. However, the N pressure, and hence arrival rate, is constant, so the islands will be slightly N deficient compared to the bulk of the film. Since we presume that  $T_c$  has a local minimum at  $x = 1$ , films made under conditions to have  $x \sim 1$  in the bulk of the film will have isolated, disconnected islands of higher- $T_c$  material at the substrate interface, and thus fulfill condition (ii).

Direct evidence for (i) comes from the behavior of the resistive transitions in a magnetic field,  $H$ . To avoid the complications of surface superconductivity, fields are applied perpendicular to the plane of the film. Some results have been shown in Figs. 3 and 4; those plus others are summarized in Fig. 9 for four samples which are at the peak in  $r_R$  versus  $P_N$  (see Fig. 1). The foot of the resistive transition for each of the four films (e.g., see Figs. 3 and 4) can be followed continuously as a function of  $H$  and they are represented by solid triangles in Fig. 9, while the midpoints of these transitions are shown as open triangles. The upper critical field slope,  $H'_{c2} \equiv -(dH_{c2}/dT)_{T_c}$ , is clearly smallest for the foot and equal to 4.2–4.5 kOe/K. Referring to Eq. (2), the cleanest (lowest  $\rho_N$ ) phase must be represented by the foot since it exhibits the lowest  $H'_{c2}$ . More disordered phases have larger  $H'_{c2}$  and are represented by, e.g., the midpoints (50%) or onsets (99%) of the resistive transitions. From assumption (ii), the low- $T_c$  foot must be the majority phase in the film. Thus, the  $T_c$  of the stoichiometric phase in our best films is 8.3–8.4 K, and this is less than the minimum (foot) values found for neighboring compositions ( $P_N$ ).

The resistive transition widths,  $\Delta T_c$ , can be understood by referring to condition (i), or the solid line of Fig. 7. Clearly, near the peak in  $T_c$  at  $\rho_N = 20 \mu\Omega$  cm, the effect of a distribution of  $\rho_N$  values within a film (for example, due to varying N concentration) will have the smallest effect on  $\Delta T_c$ . For the lowest  $\rho_N$  films, the highest (onset) temperature is due to the N-deficient isolated islands and not the well-ordered, majority component of these films. Therefore, the width of the foot of these transitions, which represent the majority of the film, are also shown in Fig. 7 as the solid rectangles. The sharpening of the resistive transitions with radiation damage is discussed at the end of Sec. V.

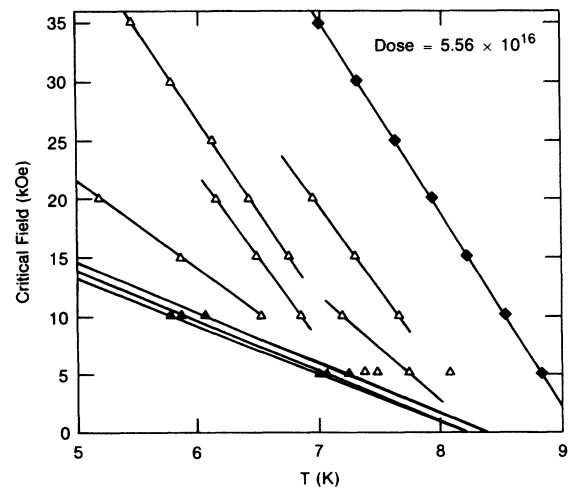


FIG. 9. Critical fields for four stoichiometric films. Solid triangles: foot of the resistive transition; open triangles: midpoints of resistive transitions; diamonds: one of the samples after irradiation to  $5.56 \times 10^{16} \alpha/\text{cm}^2$ .

## IV. SPIN FLUCTUATIONS

Any nonmonotonic variation of  $T_c$  against another physical property strongly indicates the possibility of two competing mechanisms. For example, it was recently shown<sup>15</sup> that the dip in  $T_c$  of radiation damaged Nb<sub>3</sub>Ir was consistent with a competition between increases in  $T_c$  due to increases in  $N(0)$  and decreases in  $T_c$  due to electron localization. In the present case, we will show that the peak in  $T_c$  versus  $N$  concentration,  $x$ , is consistent with a competition between the opposing effects on  $T_c$  of decreases in both the electron-phonon coupling and spin fluctuations.

Spin fluctuations have been predicted<sup>5</sup> to exhibit strong effects in VN, and are characterized by a Stoner factor,  $S$ , greater than one, where

$$S = (\chi - \chi_{\text{orb}}) / \chi_p, \quad (3)$$

where  $\chi$  is the magnetic susceptibility,  $\chi_{\text{orb}}$  is the orbital susceptibility, and the Stoner factor represents the exchange enhancement of the nonorbital spin part above the ordinary Pauli term,  $\chi_p = 2\mu_B^2 N(0)$ , where  $\mu_B$  is the Bohr magneton and  $N(0)$  is the band-structure density of states for one spin state only. Measurements of  $\chi$  as a function of  $x$  have been reported<sup>2</sup> for VN. Alternatively,  $S$  can be related to an exchange correlation integral,  $I$ , such that

$$S = \frac{1}{1 - N(0)I} \equiv \frac{1}{1 - \bar{S}}. \quad (4)$$

Various approximations have been proposed to determine the influence of spin fluctuations on  $T_c$  by introducing an interaction parameter,  $\lambda_s$ , into the Eliashberg theory. Consider the usual McMillan equation:<sup>3</sup>

$$T_c = (\omega_{\text{log}} / 1.2) \exp \left[ - \frac{1.04(1 + \lambda)}{\lambda - \mu(1 + 0.62\lambda)} \right], \quad (5)$$

where  $\lambda$  is the attractive electron-phonon coupling constant,  $\mu$  the Coulomb repulsion, and  $\omega_{\text{log}}$  is an appropriate average phonon frequency [see Eq. (10)]. Including spin fluctuations,<sup>16-18</sup> Eq. (5) is modified by using effective values of  $\lambda$  and  $\mu$  given by

$$\lambda_{\text{eff}} = \lambda / (1 + \lambda_s) \quad (6)$$

$$\mu_{\text{eff}} = (\mu + \lambda_s) / (1 + \lambda_s). \quad (7)$$

Including also  $f_1$  and  $f_2$ , the strong-coupling corrections of Allen and Dynes,<sup>4</sup> one finds

$$T_c = \frac{f_1 f_2 \omega_{\text{log}}}{1.2} \exp \left[ - \frac{1.04(1 + \lambda + \lambda_s)}{\lambda - (\mu + \lambda_s)[1 + 0.62\lambda / (1 + \lambda_s)]} \right], \quad (8)$$

and the effect of  $\lambda_s$  is to decrease  $T_c$  through the enhancement of the Coulomb repulsion term [Eq. (7)], but also by reducing the electron-phonon attractive term [Eq. (6)]. We make the customary assumption that  $\mu = 0.13$  throughout.

At  $T = 0$ , Doniach and Engelsberg<sup>19</sup> derived the relation of  $\lambda_s$  to the Stoner factor [Eq. (4)] to be

$$\lambda_s = 4.5\bar{S} \ln[1 + p^2\bar{S} / 12(1 - \bar{S})], \quad (9)$$

where  $p$  is a momentum cutoff parameter. Although this is only strictly valid within a free-electron model, it gives a definite means of connecting  $\lambda_s$  to  $S$  with a single undetermined parameter,  $p$ .

In order to make a convincing case for spin fluctuations, quantitatively, the factors in Eq. (8) must be determined as a function of  $x$  with a minimum number of adjustable parameters. Additionally, in contradistinction to the first-principles theoretical analysis of Ref. 5, we will use experimental results, whenever possible, to determine the parameters in Eq. (8).

The prefactor,  $\omega_{\text{log}}$ , is defined by

$$\ln \omega_{\text{log}} = \frac{\int_0^\infty \ln(\omega) \alpha^2 F(\omega) d \ln(\omega)}{\int_0^\infty \alpha^2 F(\omega) d \ln(\omega)}, \quad (10)$$

where  $F(\omega)$  is the phonon density of states and  $\alpha^2$  the electron-phonon coupling strength. Using Eq. (10), we find  $\omega_{\text{log}} = 254$  K from the data of Ref. 5 for stoichiometric VN. For N-deficient VN<sub>*x*</sub>, inelastic neutron scattering measurements for  $x = 0.86, 0.93$ , and  $1.0$  show<sup>20</sup> a stiffening of the acoustic spectrum as  $x$  decreases. This can be fit approximately to

$$\omega_{\text{log}}(x) = (217 \text{ K})[1 + 4.3(1 - x)]^{1/2} + 37 \text{ K}, \quad (11)$$

which is used in our calculations.

For the strong-coupling corrections,  $f_1$  and  $f_2$ , a higher moment integral of  $\alpha^2 F(\omega)$  is required. These result in a small correction ( $f_1 f_2 \sim 1.05$ ) which is computed using Ref. 3.

Because  $\chi$  has been measured<sup>2</sup> as a function of  $x$ ,  $\lambda_s(x)$  is determined from Eqs. (3), (4), and (9) by choosing an  $x$ -independent value for  $\chi_{\text{orb}}$  (or equivalently the Stoner factor for stoichiometric VN) with  $p$  the only undetermined parameter. Note the average  $N(0)$  from band-structure calculations of Refs. 1, 5, and 18 leads to  $\chi_p = 55 \times 10^{-6}$  emu/mole for stoichiometric VN. It will turn out that the results are qualitatively independent of the exact value of  $N(0)$ , and quantitatively depend only weakly on  $N(0)$ . Using the  $x$  dependence of  $N(0)$  from Ref. 1, we find

$$\chi_p(x) = \chi_p [1 - (1 - x)R], \quad (12)$$

where  $R \cong 1.1$ . Thus,  $S(x)$  can be determined from Eq. (3), and  $S(x = 1)$  is then restricted by the values of  $\chi(x)$ ,  $\chi_p$ , and to a lesser extent  $R$ , to the range  $3.1 \leq S(x = 1) \leq 4.45$ .

The evaluation of  $\lambda$  is more complicated. In many  $A-15$  superconductors, it is found that  $\lambda$  is proportional to  $N(0)$ , independent of differences in the phonon frequencies. On the other hand, Reitschel *et al.*,<sup>5</sup> point out that the acoustic phonons stiffen<sup>20</sup> as  $x$  decreases and have used this information to calculate  $\lambda$  for  $x = 0.86, 0.93$ , and  $1.0$ . However, if their values of  $\lambda = 1.54$  for stoichiometric VN and  $\omega_{\text{log}}$  are used in Eq. (8), a much smaller value of  $\lambda_s \cong 0.25$  than their value of  $0.54$  is needed to get the experimental  $T_c$ . One can argue whether the procedures of Ref. 5 are superior to Eq. (8), but

Daams *et al.*<sup>16</sup> make a strong case for Eq. (8), and we must use it since our analysis does not involve microscopic calculations. It could also be argued that the stiffening of the lattice *results* from the decrease in  $N(0)$ , as  $x$  decreases, due to the effects of conduction electrons on the elastic properties (see Ref. 21).

To determine  $\lambda(x)$ , we interpolate between values determined from experimental  $T_c$  measurements at  $x = 1$  and for  $x \leq 0.85$ , where  $\chi(x)$  and therefore  $\lambda_s(x)$  do not vary much. Given values of  $\chi_{orb}$  and  $\chi_p$ , which are assumed to be independent of  $x$ , and the calculated<sup>1</sup>  $N(0)$  as a function of  $x$ , then  $\lambda_s(x)$  is fully determined. Then from the experimental values of  $T_c(0.75) = 2.2$  K,  $T_c(0.85) = 5.25$  K determined from measurements<sup>2,4</sup> on bulk samples and  $T_c(1.0) = 7.8$  K, determined from an extrapolation of results on radiation damaged stoichiometric films to the pure ( $\rho_N = 0$ ) limit (see next section), the values of  $\lambda(x)$  for  $x = 0.75, 0.85$ , and  $1.0$  are easily found using Eq. (8). These values are interpolated to intermediate  $x$  values by a second-order polynomial fit. It turns out that the specific values of  $\chi_{orb}$  and  $N(0)$  are not so important, but  $p$  determines the magnitude of  $\lambda_s$  through Eq. (9). Finally, the proper value of  $p$  is chosen so that the peak in calculated  $T_c(x)$  is equal to our measured value of 8.9 K.

Summarizing what we have done so far,  $T_c(x)$  can be determined, given various experimental data [ $T_c(x = 1)$ ,  $\chi(x)$ ,  $\omega_{log}(x)$ ,  $f_1, f_2$ ], the calculated  $N(0)$  as a function of  $x$ , and the guessed values of  $p$  and  $\chi_{orb}$ , or equivalently  $S(x = 1)$ . It should be emphasized that while  $\lambda(x)$  is empirically determined, the value of  $\lambda_s$  is found from the single adjustable parameter,  $p$ , which is fixed by fitting the peak value of  $T_c(x)$  at 8.9 K data. For any allowed value of  $S(x = 1)$ , we find  $p \sim 0.4$ . The result for  $S(x = 1) = 3.5$  is shown in Fig. 7 together with the experimental data. Note that the peak in calculated  $T_c$  occurs for  $x \approx 0.96$ , in good agreement with the estimate based on lattice constant (see Sec. II). In plotting the calculated curve in Fig. 7, the calculated peak position ( $x = 0.96$ ) is adjusted to coincide with the measured peak position ( $\rho_N = 18 \mu\Omega \text{ cm}$ ), and  $\rho_N$  is assumed to be proportional to  $(1 - x)$ . This proportionality may break down for higher values of  $\rho_N$  but reflects the fact that N vacancies will act as strong scattering centers. Note that the fit is forced to agree with the bulk results of  $T_c(0.85) = 5.25$  K and  $T_c(0.75) = 2.2$  K by our procedure to determine  $\lambda(x)$ .

Although this fit does not strongly depend on  $S(x = 1)$ , the parameters  $\lambda$  and  $\lambda_s$  for stoichiometric VN do, and they are plotted against  $S(x = 1)$  in Fig. 10. The  $T_c$ , in the absence of spin fluctuations (i.e., with  $\lambda_s = 0$ ), for the  $\lambda$  values shown in Fig. 10, increases with  $S(x = 1)$  from  $\sim 14$  to 21.6 K. Also note that  $\chi_{orb}$  decreases linearly in this model from  $80 \times 10^{-6}$  emu/mole at  $S(x = 1) = 3$  to zero at  $S(x = 1) = 4.45$ . We have no additional experimental evidence to make a choice between these, but an independent determination of  $\chi_{orb}$  could fix  $S(x = 1)$ . Calculated values of  $S(x = 1)$  range from<sup>5</sup> 2.9 to<sup>22</sup> 3.9.

On the whole, we feel this qualitative and semiquantitative agreement adequately demonstrates the compatibility of the spin fluctuation model with our results on N-

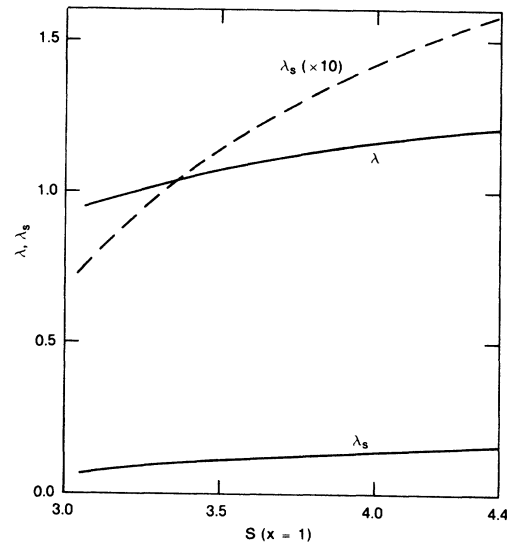


FIG. 10. The variation of the electron-phonon coupling,  $\lambda$ , and the spin fluctuation coupling,  $\lambda_s$ , for stoichiometric VN as a function of the Stoner factor  $S(x = 1)$  for stoichiometric VN based on the model presented in the text.

deficient VN<sub>x</sub>. This was uniquely possible for VN<sub>x</sub> because measurements and/or calculations of  $\chi$ ,  $\alpha^2F(\omega)$ , and  $N(0)$  were available as a function of  $x$ . It should also be noted, however, that the effect of spin fluctuations found here is smaller than previously suggested<sup>5</sup> for VN.

## V. RADIATION DAMAGE

Irradiation with 1.8 meV  $\alpha$  particles of a series of stoichiometric (high  $r_R$ ) films was done at the Argonne Dynamitron facility. This energy and the film thickness of  $0.5 \mu\text{m}$  were chosen so that the  $\alpha$  particles would penetrate deep into the substrate and leave a uniform damage profile in the VN. Starting with a set of five films made together, one was used for susceptibility measurements, one kept as an unirradiated standard, and the others progressively irradiated to doses of  $1-20 \times 10^{16}$   $\alpha/\text{cm}^2$ . These films were on  $0^\circ$  substrates so that x-ray diffraction was possible and a full set of superconducting measurements were conducted after each irradiation as well as on the virgin films. As shown in Fig. 4, the resistive transitions sharpened with irradiation. Because of the discussion of the previous section, we have followed the behavior of the foot of the transition in order to isolate the stoichiometric, majority phase of these films. The results for  $T_c$  and  $H'_{c2}$  are shown in Figs. 11 and 8 (open circles) as a function of  $\rho_n$ . The cluster of four data points as lowest  $\rho_n$  are the films before irradiation. It was found that  $\rho_n$  increased approximately linearly with  $\alpha$ -particle dose up to  $24 \mu\Omega \text{ cm}$  for  $5.6 \times 10^{16}$   $\alpha/\text{cm}^2$ . However, in going from  $10$  to  $20 \times 10^{16}$   $\alpha/\text{cm}^2$ ,  $\rho_n$  increased dramatically to  $\sim 63 \mu\Omega \text{ cm}$  and the film had an uneven visual appearance, suggestive of bubbles of helium gas forming in the substrate and cracking the surface. For this sample,  $T_c$  fell to 8.26 K and  $H'_{c2}$  rose to 23 kOe/K,

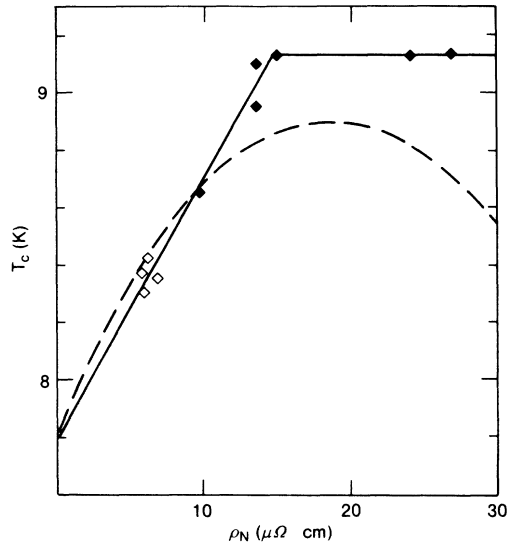


FIG. 11. The variation of  $T_c$  vs  $\rho_N$  for the foot of the transition of radiation damaged samples of stoichiometric VN (solid diamonds). Open diamonds: samples before irradiation; solid line: extrapolation of  $T_c$  to  $\rho_N=0$ ; dashed line: calculated  $T_c$  vs  $\rho_N$  of substoichiometric  $VN_x$  films for comparison (see Fig. 7).

but the interplay of the new type of disorder from substrate cracks makes the interpretation difficult. Further analysis does not include this highest dose sample.

In Fig. 11,  $T_c$  is seen to increase linearly, but then abruptly saturates at  $\sim 9.13$  K. Although this could be interpreted as a saturation of our ability to further damage the film due to spontaneous recombination of defects,<sup>23</sup> the continuing increase of  $H'_{c2}$  and decrease of  $r_R$  implies this is not the case. From the data of Fig. 11, the values of  $T_c$  can be extrapolated to the pure ( $\rho_n=0$ ), stoichiometric limit yielding a value of  $7.8 \pm 0.1$  K. This is the origin of the value used in fitting to the spin-fluctuation model in Sec. IV.

Likewise, the  $H'_{c2}$  values shown in Fig. 8 are extrapolated to a stoichiometric clean limit giving a value of  $600 \pm 200$  Oe/K. However, it is clear that the slope of  $H'_{c2}$  versus  $\rho_n$  falls significantly above the prediction of the GLAG theory [Eq. (2)] using the experimental Sommerfeld constant and is in reasonable agreement with the substoichiometric samples.

Results for the lattice constant variation with irradiation are shown in Fig. 12, together with unirradiated samples which includes nonstoichiometric samples. The general result is that the lattice constant increases with N content and with damage. The stoichiometric, undamaged value of  $4.157$  Å is significantly larger than the accepted bulk value of  $4.136$  Å, but thin films often exhibit expanded lattices.

Finally, the sharpening of the resistive transitions with radiation damage, especially in a field (see Fig. 4), can be understood qualitatively. The damage will have a relatively stronger effect on the clean, majority component of stoichiometric films than on the already disordered, higher- $T_c$  regions. For example, differences in  $T_c$  and

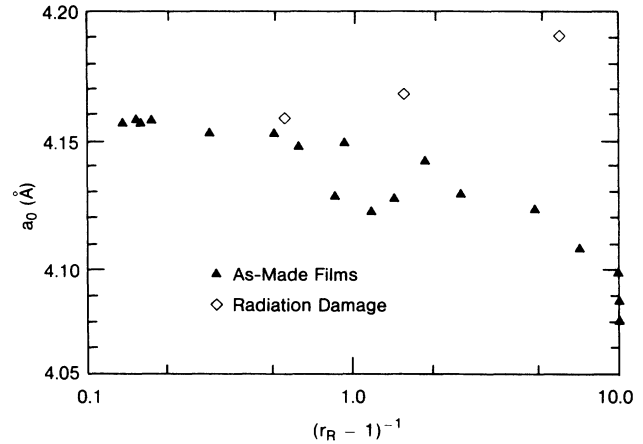


FIG. 12. Lattice constant determined from x-ray diffraction as function of  $(r_R - 1)^{-1}$  for "as-made" films (solid triangles) and radiation damaged stoichiometric films (open diamonds).

$H'_{c2}$  values for these components will decrease and thus the resistive transitions become sharper, and stay so in a field.

## VI. SUMMARY

The major new experimental discovery is that  $T_c$  exhibits a local minimum for pure ordered and stoichiometric VN. Small deviations off stoichiometry lead to increases in  $T_c$  and so does disordering of stoichiometric VN by mild radiation damage with  $\alpha$  particles. When the N vacancies or  $\alpha$ -particle dose becomes sufficiently large  $T_c$  goes through a peak and then falls. While it is tempting to describe this as purely a disorder effect, such a description ignores the decrease in conduction electron density when N is removed.<sup>2</sup>

Instead, we have considered, for the case of N vacancies, the competition between spin fluctuations and electron-phonon coupling on  $T_c$ . A semiquantitative model was described in which both the electron-phonon coupling,  $\lambda$ , and the spin fluctuation coupling,  $\lambda_s$ , decreased with increasing N vacancies. Since they have opposite effects on  $T_c$ , one expects a nonmonotonic variation of  $T_c$  with  $x$ . Using primarily experimental data, we showed that this model can reproduce  $T_c(x)$  quite satisfactorily. A key ingredient was the sharp decrease in  $\chi$  as  $x$  decreased from one.

The open question is how to understand the similar increase in  $T_c$  with disorder due to  $\alpha$ -particle damage of stoichiometric VN. In this case, there are no measurements of  $\chi$ ,  $\alpha^2 F(\omega)$  nor calculations of  $N(0)$  known to us, to base a similar analysis. It is possible that the decreases in spin fluctuations in substoichiometric  $VN_x$  are primarily due to disorder and therefore would be expected to occur for disorder induced by radiation damage. However, there is no direct evidence for this from experimental measurements of  $\chi$ , and in general the effects of strong disorder are to enhance the Coulomb interaction,<sup>24</sup> and hence, presumably, spin fluctuations. Further work is needed to resolve this issue.

The studies of superconducting properties in  $\alpha$ -particle

disordered stoichiometric VN has allowed us to extrapolate these to pure ( $\rho_N=0$ ) stoichiometric VN and we find  $T_c=7.8\pm 0.1$  K;  $H'_{c2}=600\pm 200$  Oe/K; and  $\langle v_F^* \rangle=2.4 (\pm 0.4)\times 10^7$  cm/sec from Eq. (15) of Ref. 15. However, we also find that the variation of  $H'_{c2}$  with  $\rho_N$  shows a significant disagreement with the GLAG theory if the experimentally measured Sommerfeld constant is used.

X-ray diffraction shows that the lattice constant increases with  $N$  content  $x$ , and also with  $\alpha$ -particle dose. Both of these are in agreement with expectations, and so is the significantly larger lattice constant for sputtered films compared to bulk.

In plotting the measured  $\rho_N$  against  $(r_R-1)$  we found a good power law (exponent  $\approx -0.59$ ) over the full range, but we found neither the expected inverse law (ex-

ponent  $= -1$ ) in the clean limit nor the saturation at a maximum metallic resistivity in the dirty limit. Perhaps the result is significant, or perhaps we have just not achieved these limits.

#### ACKNOWLEDGMENTS

We would like to thank Scott Chumbley for preparation of specimens for transmission electron microscopy (TEM) and subsequent analysis, Andrew Wagner for measuring film thicknesses, and D. S. Gemmell and B. J. Zabransky for the use and operation of the Dynamitron radiation facility. This work was supported by the U.S. Department of Energy, Division of Basic Energy Sciences—Materials Sciences, under Contract No. W-31-109-ENG-38.

- 
- <sup>1</sup>P. Marksteiner, P. Weinberger, A. Neckel, R. Zeller, and P. H. Dederichs, *Phys. Rev. B* **33**, 812 (1986).
- <sup>2</sup>F. I. Ajami and R. K. MacCrone, *J. Phys. Chem. Solids* **36**, 7 (1975).
- <sup>3</sup>W. L. McMillan, *Phys. Rev.* **167**, 331 (1968).
- <sup>4</sup>P. B. Allen and R. C. Dynes, *Phys. Rev. B* **12**, 905 (1975).
- <sup>5</sup>H. Rietschel, H. Winter, and W. Reichardt, *Phys. Rev. B* **22**, 4284 (1980).
- <sup>6</sup>J. Zasadzinski, R. Vaglio, G. Rubino, K. E. Gray, and M. Russo, *Phys. Rev. B* **32**, 2929 (1985).
- <sup>7</sup>G. Brauer and W. D. Schnell, *J. Less-Common Met.* **6**, 326 (1964).
- <sup>8</sup>W. Lengauer and P. Ettmayer, *J. Less-Common Met.* **109**, 351 (1985).
- <sup>9</sup>B. R. Zhao, L. Chen, H. L. Luo, M. D. Jack, and D. P. Mullin, *Phys. Rev. B* **29**, 6198 (1984).
- <sup>10</sup>W. K. Schubert, R. N. Shelton, and E. L. Wolf, *Phys. Rev. B* **23**, 5097 (1981).
- <sup>11</sup>A. F. Ioffe and A. R. Regel, *Prog. Semicond.* **4**, 237 (1960); P. B. Allen, in *Superconductivity in d- and f-band Metals*, edited by H. Suhl and M. B. Maple (Academic, New York, 1980), p. 291.
- <sup>12</sup>T. P. Orlando, E. J. McNiff, Jr., S. Foner, and M. R. Beasley, *Phys. Rev. B* **19**, 4545 (1979).
- <sup>13</sup>C. Geibel, H. Rietschel, A. Junod, M. Pelizzone, and J. Muller, *J. Phys. F* **15**, 405 (1985).
- <sup>14</sup>W. Lengauer, *J. Phys. Chem. Solids* (in press).
- <sup>15</sup>K. E. Gray, R. T. Kampwirth, T. F. Rosenbaum, S. B. Field, and K. Muttalib, *Phys. Rev. B* **35**, 8405 (1987).
- <sup>16</sup>J. M. Daams, B. Mitrovic, and J. P. Carbotte, *Phys. Rev. Lett.* **46**, 65 (1981).
- <sup>17</sup>M. A. Jensen and K. Andres, *Phys. Rev.* **165**, 545 (1968); G. Riblet, *Phys. Rev. B* **3**, 91 (1971).
- <sup>18</sup>M. Dacorogna, T. Jarlborg, A. Junod, M. Pelizzone, and M. Peter, *J. Low Temp. Phys.* **57**, 629 (1984).
- <sup>19</sup>S. Doniach and S. Engelsberg, *Phys. Rev. Lett.* **17**, 750 (1966).
- <sup>20</sup>W. Weber, P. Roedhammer, L. Pintschovius, W. Reichardt, F. Gompf, and A. N. Christensen, *Phys. Rev. Lett.* **43**, 868 (1979).
- <sup>21</sup>M. Grimsditch, K. E. Gray, R. Bhadra, R. T. Kampwirth, and L. Rehn, *Phys. Rev. B* **35**, 883 (1987).
- <sup>22</sup>D. A. Papaconstantopoulos, W. E. Pickett, B. M. Klein, and L. L. Boyer, *Phys. Rev. B* **31**, 752 (1985).
- <sup>23</sup>H. Wenzl, in *Vacancies and Interstitials in Metals*, edited by A. Seeger, D. Schumacher, W. Schilling, and J. Diehl (North-Holland, Amsterdam, 1970), p. 391.
- <sup>24</sup>B. L. Altschuler, A. G. Aronov, and P. A. Lee, *Phys. Rev. Lett.* **44**, 1288 (1980).